A simple stochastic model for cell population dynamics in colonic crypts

Konstantinos Mamis[a], Ruibo Zhang[a], and Ivana Bozic*[a]

[a]Department of Applied Mathematics, University of Washington, Seattle, WA 98195, USA

Abstract

The questions of how healthy colonic crypts maintain their size, and how homeostasis is disrupted by driver mutations, are central to understanding colorectal tumorigenesis. We propose a three-type stochastic branching process, which accounts for stem, transit-amplifying (TA) and fully differentiated (FD) cells, to model the dynamics of cell populations residing in colonic crypts. Our model is simple in its formulation, allowing us to easily estimate all but one of the model parameters from the literature. Fitting the single remaining parameter, we find that model results agree well with data from healthy human colonic crypts, capturing the considerable variance in population sizes observed experimentally. Importantly, our model predicts a steady state population in healthy colonic crypts for relevant parameter values. We show that *APC* and *KRAS* mutations, the most significant early alterations leading to colorectal cancer, result in increased steady-state populations in mutated crypts, in agreement with experimental results. Finally, our model predicts a simple condition for unbounded growth of cells in a crypt, corresponding to colorectal malignancy. This is predicted to occur when the division rate of TA cells exceeds their differentiation rate, with implications for therapeutic cancer prevention strategies.

1 Introduction

The epithelial inner surface of the human colon exhibits about 10^7 to 10^8 column-like invaginations [1], called crypts, each one of which contains ~ 2000 cells [2, 3]. In order to maintain their total size, mature colonic crypts are in homeostatic steady-state, where the cell proliferation in the lower part of the crypt is in equilibrium with the cell loss due to apoptosis [3, 4, 5]. Depending on their proliferation capability, cells in colonic crypts are identified as stem, transit-amplifying (TA), or fully differentiated (FD) [4, 6]. In the base of the crypt column resides a small population of about 15 stem cells [7, 8]. Stem cells divide on average once a day [7, 9, 10], producing cells that are transit-amplifying. Cell proliferation in colonic crypts is largely maintained by the TA cells, which divide every 12 to 16 hours [6, 10, 11] while they migrate upward, towards the crypt lumen. After undergoing several rounds of divisions [6, 12], they lose their proliferation capability, resulting in fully differentiated cells [9, 13]. Finally, FD cells undergo apoptosis and are shed into the intestinal lumen [5, 14]. Except for the stem cells, the total lifespan of epithelial cells, from crypt base to lumen, is 3 to 5 days [15], making the intestinal epithelium one of the most rapidly renewing tissues in the human body.

So far, many models have been proposed for the cell population dynamics in a crypt [16], with a lot of works focusing on stem cell dynamics in particular [17]. Cell population models for crypts broadly fall into two categories: spatial and compartmental models. Spatial models are based on the fact that the proliferation capability of each cell diminishes gradually as it moves upwards in the crypt, and they typically take the stochasticity of cell dynamics into account [3, 18, 19, 20, 21]. The main drawback of spatial models is their high level of complexity, since they may include the cell proliferation gradient along crypt's vertical axis [3, 18], a detailed description of the cell mitotic cycle [19, 20, 21], cell mobility [20] or Wnt signalling [21]; however for the parameters of these processes, estimation from experimental measurements is not straightforward. Thus, spatial models are particularly useful in deducing qualitative results or testing different hypotheses concerning the mechanisms of cell dynamics, rather than making quantitative predictions for the cell populations in a crypt.

*Corresponding author: ibozic@uw.edu

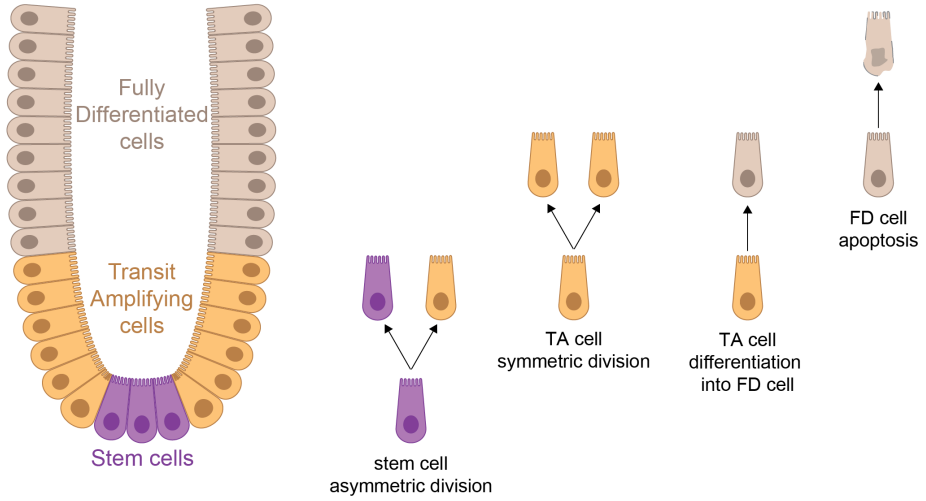

Figure 1: Schematic representation of cell populations and cell dynamics in a colonic crypt.

Compartmental models, on the other hand, do not make use of the spatial character of cell proliferation, describing instead the progression of cells through the different compartments that constitute the total cell population in a crypt. Most of compartmental models are deterministic [4, 22, 23, 24], and thus cannot capture the variability in cell populations within the crypt, which is significant [2, 3, 18, 25]. Compartmental models have been mainly employed to describe the mechanisms in cell population dynamics that result in homeostasis, their stability, and possible ways they can be disrupted resulting in tumorigenesis [2, 4, 26]. Of particular interest are feedback control mechanisms between different populations of cells [2, 4, 24]. However, most of the results are qualitative, since the values of model parameters remain unspecified [4, 24, 26]. More detailed compartmental models may contain more compartments corresponding to different phases of cell cycle [22, 27], or incorporate both stochasticity and control networks between the different cell compartments [2]. However, most of their parameters are not estimated directly from experimental measurements; rather, parameter values are adjusted so that model simulations are able to reproduce experimental data, such as the distribution of proliferative cells along the crypt axis, or the averages and variances of cell populations in a crypt.

In the present work, we propose the branching process depicted schematically in Fig. 1, as a new stochastic model for cell dynamics in a colonic crypt that **i)** is minimal and simple in its formulation, which allows us to directly estimate all model parameters except for one, **ii)** is able to model the cell population dynamics in both healthy and mutated colonic crypts, **iii)** its solution is obtained analytically. More specifically, for healthy crypts, our model explains both the attainment of homeostatic steady-state and the variability in cell population sizes from crypt to crypt. Furthermore, our model describes the increase in size of mutant crypts [25], by considering the effects on cell properties of the most common mutations found in early stages of colorectal tumorigenesis, such as *APC* and *KRAS* [11, 28, 29]. Its analytic solution is another significant aspect of the model, as it provides a simple mathematical description of the homeostatic mechanisms inside a colonic crypt and the disruption thereof, shedding light on the mechanisms that result in colorectal tumorigenesis.

Branching processes have been used to model cell population dynamics [30], with applications in the study of mutation acquisition in cancer progression [31, 32, 33, 34], tumor progression and ctDNA shedding [35], and epidermal homeostasis [36]. In particular, epidermal homeostasis was successfully described by using an exactly solvable, two-type branching process for cell dynamics [36, 37]. Our model is another example of describing a homeostatic mechanism in healthy tissue by a branching process. From its solution, we are able to determine the steady-state distributions of different cell population sizes in a crypt, as well as exact formulas for their averages and variances.

For the model parameters of stem cell number, stem and TA cell division rates and FD cell apoptosis rate, we use typical values found in the literature on healthy human colonic crypts. Since no such direct value estimation was found for TA differentiation rate into FD cells, we estimate it from the average crypt size observed in humans. While we estimate only one parameter using the average crypt size, our model predicts distributions for TA, FD, and total cell populations that are in good agreement with experimental

data [2, 3], encapsulating the stochasticity of cell dynamics in a crypt. We also consider the changes in values of model parameters, resulting from the *APC* and *KRAS* mutations that are commonly found in early stages of colorectal tumorigenesis. We show that our model is able to capture the changes in size and population structure of mutant crypts demonstrated experimentally.

2 Model

We propose a continuous-time branching process with three types, corresponding to stem (S), transit-amplifying (TA) or fully differentiated (FD) cells, to model population dynamics in a colonic crypt. In this stochastic model depicted in Fig. 1, cells undergo divisions, differentiations and apoptoses with constant rates but at random times. We describe this branching process by the rate equations

$$\begin{aligned} &\mathrm{S} \xrightarrow{r} \mathrm{S\ TA} \\ &\mathrm{TA} \xrightarrow{\lambda} \mathrm{TA\ TA} \\ &\mathrm{TA} \xrightarrow{d} \mathrm{FD} \\ &\mathrm{FD} \xrightarrow{\gamma} \emptyset. \end{aligned} \tag{1}$$

In the model, the number N_0 of stem cells per crypt remains constant, since we consider that stem cells only divide asymmetrically with rate r, producing one stem and one TA cell. Recent research [1, 38] has challenged the previously held position that stem cells divide predominantly asymmetrically. Each stem cell is thought to divide symmetrically into two daughter stem cells most of the time, with asymmetry being controlled on the population level: Stemness is a property of cells residing in the stem cell niche in colonic crypt base [7, 9], and each symmetric division results in one surplus stem cell being pushed upwards, differentiating into a TA cell [8, 39]. This mechanism results in the tight regulation of stem cell numbers per crypt, which in turn allows us to assume, in our model, that stem cells *effectively* undergo asymmetric divisions, as each stem cell division ultimately results in one new TA cell.

The proliferating compartment of the crypt consists mainly of the TA cell population. TA cells are rapidly-cycling, undergoing a number of cell divisions before their final differentiation [6]. In our model, TA cell behavior consists of symmetric division with rate λ, or differentiation into an FD cell with rate d. Note that cell proliferation capability depends on the location of the cell along the crypt axis, since it is controlled by signaling factors whose concentration decreases as cells move away from the crypt base [1]. Thus, in our model we assume that TA differentiations occur independently of TA divisions [40].

Last, FD cells, having lost their proliferation capability, can only undergo apoptosis with rate γ.

2.1 Average sizes of cell populations and condition for homeostasis

We formulate a system of ordinary differential equations that describes the time evolution of average population sizes of TA and FD cells, denoted as $m_{\mathrm{TA}}(t)$ and $m_{\mathrm{FD}}(t)$ respectively:

$$\begin{aligned} m'_{\mathrm{TA}}(t) &= rN_0 + (\lambda - d)m_{\mathrm{TA}}(t) \\ m'_{\mathrm{FD}}(t) &= d\, m_{\mathrm{TA}}(t) - \gamma\, m_{\mathrm{FD}}(t). \end{aligned} \tag{2}$$

Under condition

$$d > \lambda, \tag{3}$$

and regardless of the initial cell populations, system of equations (2) attains a steady state; that is, for large times that exceed the cell turnover timescale, the average TA and FD cell populations remain constant and equal to

$$m_{\mathrm{TA}} = \frac{rN_0}{d-\lambda}, \quad m_{\mathrm{FD}} = \frac{d}{\gamma} m_{\mathrm{TA}}. \tag{4}$$

Thus, under condition (3), the crypt maintains a finite size, which, on average, is equal to

$$N_{\mathrm{tot}} = N_0 + m_{\mathrm{TA}} + m_{\mathrm{FD}} = \left[1 + \frac{r}{d-\lambda} + \frac{rd}{\gamma(d-\lambda)}\right] N_0. \tag{5}$$

On the other hand, if condition (3) is violated, system (2) predicts an unbounded growth of both TA and FD cell numbers. Thus, stationarity condition $d > \lambda$ provides us with a simple description of the homeostasis

for crypt size: In order for the crypt to maintain its finite size, TA cell division has to be regulated, with TA division rate λ being less than rate d of TA differentiation into FD cells. While we derived the stationarity condition for the averaged Eqs. (2), it is also the stationarity condition for the stochastic population model (1).

2.2 Probability distribution for number of TA and FD cells

Moving now to the stochastic setting of model (1), we explicitly determine the exact steady-state probability distribution for the number of TA cells per crypt: For large times, the number of TA cells follows a generalized negative binomial distribution, with the number of successes being rN_0/λ and success probability $(d-\lambda)/d$ (Supplementary Information, section S3). In other words, probability that the number of TA cells is equal to n_1 is given by

$$P_{n_1} = \frac{\Gamma(n_1 + (rN_0/\lambda))}{n_1!\Gamma(rN_0/\lambda)} \left(\frac{d-\lambda}{d}\right)^{rN_0/\lambda} \left(\frac{\lambda}{d}\right)^{n_1}, \quad n_1 = 0, 1, 2, \ldots, \tag{6}$$

where $\Gamma(\cdot)$ is the gamma function. The average number of TA cells, as calculated from distribution (6), agrees with the result (4) we obtained from the averaged deterministic problem, while the variance of TA cell population reads

$$\sigma^2_{\mathrm{TA}} = \frac{rdN_0}{(d-\lambda)^2}. \tag{7}$$

Furthermore, by making use of FD cell dynamics, in combination with the known distribution P_{n_1} for the TA cell population, we formulate the following approximation for the steady-state distribution of the number n_2 of FD cells (see Supplementary Information, section S4):

$$P_{n_2} \approx \sum_{n_1=0}^{\infty} P_{n_1} \frac{(dn_1/\gamma)^{n_2}}{n_2!} e^{-dn_1/\gamma}. \tag{8}$$

Approximation (8) is easily computable, and we show its accuracy in Fig. 3, for model parameters corresponding to healthy human colonic crypts.

2.3 Probability distribution for total number of cells in a crypt

In order to determine the steady-state distribution of the total number of cells per crypt, we formulate and solve the Kolmogorov equation corresponding to branching process (1) (Supplementary Information, section S5). From its solution, we derive the exact distributions for TA, FD and total cell populations in a crypt (Supplementary Information, section S6). The exact distributions for cell populations agree with the results obtained from direct Gillespie simulations of the model (Supplementary Information, Fig. S1).

From the exact solution, we derive closed form formulas for the variance for the number of FD cells

$$\sigma^2_{\mathrm{FD}} = \frac{rN_0}{\lambda}\left[\frac{B}{\alpha} + \frac{B^2}{\alpha^2(\alpha+1)}\right], \tag{9}$$

where $\alpha = (d-\lambda)/\gamma$, $B = \lambda d/\gamma^2$, and the covariance between the TA and FD cell populations

$$\mathsf{Cov}(\mathrm{TA}, \mathrm{FD}) = \frac{\lambda}{\gamma + d - \lambda}\sigma^2_{\mathrm{TA}}. \tag{10}$$

From these results and the variance of TA cell population, we calculate the variance of the total cell population in a crypt:

$$\sigma^2_{\mathrm{tot}} = \frac{\gamma + d + \lambda}{\gamma + d - \lambda}\sigma^2_{\mathrm{TA}} + \sigma^2_{\mathrm{FD}}. \tag{11}$$

2.4 Maintaining homeostasis under different apoptosis rates

Apoptosis rate of FD cells γ is the parameter with the greatest uncertainty in the model; estimations for FD cell lifespan vary from less than a day up to 3 days. Our model is able to efficiently attain homeostasis (i.e. maintain a constant crypt size distribution) for different FD apoptosis rates γ, by adjusting TA differentiation rate d. To show this, we consider different values for γ, and for each one of these we adjust d so that the

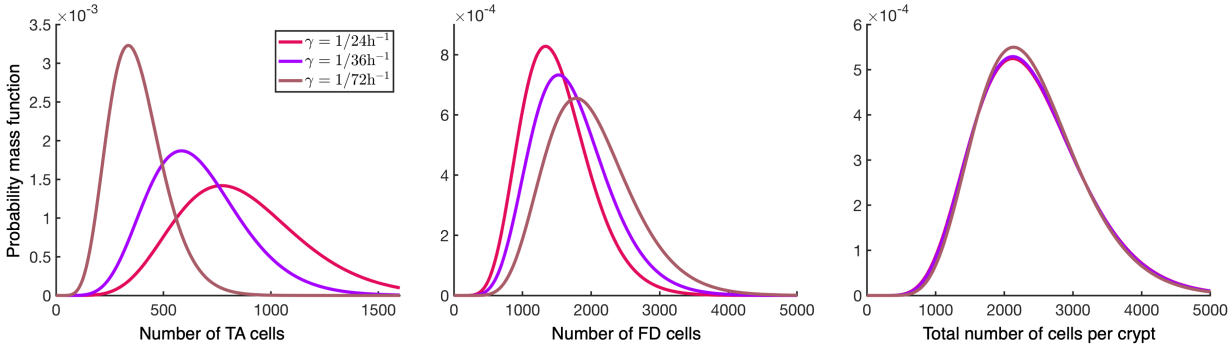

Figure 2: Crypts can maintain homeostatic size distribution under varying apoptosis rates. Steady-state probability distributions of TA, FD, and total cell populations in colonic crypts, for different apoptosis rates γ, determined by the solution of branching process (1). Values for parameters N_0, r, λ are described in Section 3, and d is adjusted to keep the average crypt size constant.

average crypt size stays ~ 2400 cells. We see in Fig. 2 that this adjustment in d results not only in keeping the average crypt sizes constant, but also leaves the crypt size distribution effectively unaltered. This is achieved by the simultaneous adjustment of the distributions for TA and FD cells: An increase in apoptosis rate γ results in an increase in the average size and variance of TA cell population and a simultaneous decrease in the FD cell population, while a decrease in γ has the opposite results. These changes in TA and FD cell populations are in agreement with the remark by Potten and Loeffler [41] that a large TA cell population is needed when cell turnover is high, i.e. for increased apoptosis rates γ; if γ is low, the tissue could in principle be maintained with just stem and FD cells.

3 Comparison of model results to experimental data

For the comparison to data, we calibrate model (1) with the following parameter values. The number of stem cells per crypt N_0 and the division rates r, λ of stem and TA cells are estimated directly from the literature; $N_0 = 15$ [7, 8], $r = 1/24\text{h}^{-1}$ since stem cells divide once every day [7, 9, 10], and $\lambda = 1/14\text{h}^{-1}$ since TA cells divide every 12 to 16 hours [6, 10, 11]. Considering that the total lifespan of a colonic epithelial cell is 3 to 5 days [15], and that its final differentiation occurs after the first 2 to 3 days [12], the average time from final differentiation to apoptosis is 1.5 days; thus we consider $\gamma = 1/36\text{h}^{-1}$ for FD apoptosis rate. Last, we found no direct estimation in the literature for the rate d of TA cells differentiation into FD cells. We treat d as a fitting parameter for our model, so that the average total size N_{tot} of the crypt is ~ 2400 cells, matching experimental observations [2, 3]. This is performed by using Eq. (5) for average crypt size, resulting in the value $d = 0.0724\text{h}^{-1}$. A similar fitting has been performed for a deterministic compartmental model for cell dynamics in hematopoiesis [23].

We compare our model predictions with the data from 49 colorectal crypts obtained from human biopsy specimens [2, 3]. In Table 1, we compare results for average sizes and variances of TA, FD, and total cells

Table 1: Comparison of sizes of cell populations in healthy human colonic crypts from model and experimental data.

Cell type	Average	Variance	CV%*
TA cells (data)	608.9	$5.5 \cdot 10^4$	38.4
TA cells (model)	659.3	$5 \cdot 10^4$	34
FD cells (data)	1768.2	$1.9 \cdot 10^5$	24.6
FD cells (model)	1717.8	$3.3 \cdot 10^5$	33.3
total number of cells (data)	2392.1	$2.4 \cdot 10^5$	20.5
total number of cells (model)	2392.1	$6.3 \cdot 10^5$	33.2

*Coefficient of variation (CV%) is the ratio of the standard deviation to average, expressed as percentage.

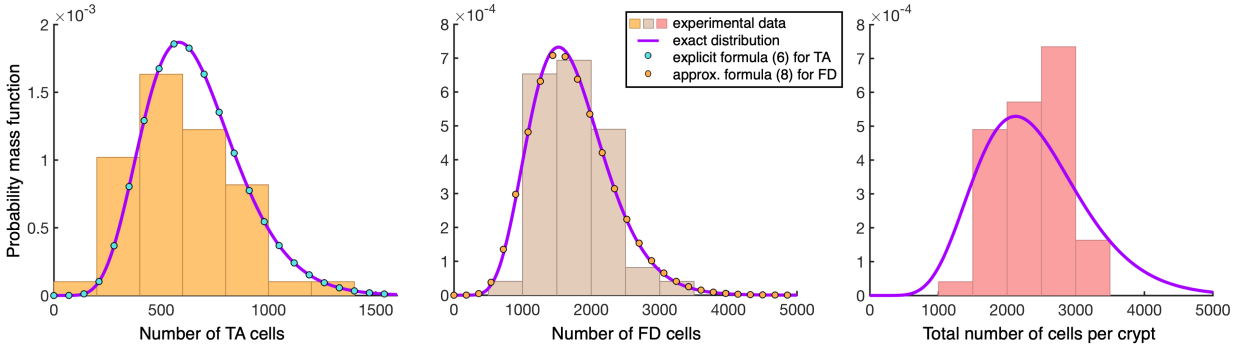

Figure 3: Comparison between experimental data and model results. Steady-state probability distributions of TA, FD, and total cell populations in healthy human colonic crypts. Histograms represent experimental data [3]. Purple curves are the exact distributions determined by the solution of branching process (1). The explicit formula (6), and the approximate formula (8), for TA and FD cell populations respectively, are denoted by circles in the first and second panels.

per crypt, to the corresponding values from the experimental data set. In Fig. 3, we show the model results for probability distributions of cell populations, along with the histograms of the experimental data, and we observe that they are in good agreement. More specifically, by performing the chi-square goodness of fit test at 5% significance level (Supplementary Information, section S7), we find that the data are consistent with the distributions predicted by our model. The agreement between the theoretical predictions of the model and the size distributions of the three cell populations (TA, FD and total number of cells) is all the more striking if we recall that it relies on fitting only a single parameter.

The main discrepancy between our model results and data from [3] is the correlation between the TA and FD cell populations. Pearson's correlation coefficient, as calculated from data, is $\rho^{\text{data}}_{\text{TA,FD}} = -0.01$, while the model predicts $\rho^{\text{model}}_{\text{TA,FD}} = 0.97$. The observation that numbers of TA and FD cells are uncorrelated has been attributed to a feedback mechanism in cell population dynamics [2]. In our model, the correlation between TA and FD cell populations can be reduced significantly if we allow apoptosis rate γ to vary randomly from crypt to crypt. More specifically, by considering FD cell lifespan in each crypt to follow a continuous uniform distribution between 12 and 60h (thus having an average of 1.5 days), and keeping the average crypt size constant, correlation coefficient is reduced to $\rho_{\text{TA,FD}} = 0.37$, while the cell population distributions stay close to the experimental data. Moreover, the distributions for total numbers of cells, as predicted by the model for constant and varying γ, effectively coincide (see Supplementary Information, Fig. S2).

On the other hand, the proportional growth between total crypt size and the proliferative cell compartment has been experimentally observed [42], and has also been incorporated in spatial crypt models [18]. This experimental result is in agreement with the positive linear dependence between TA and total cell population in our model. The reason for such potentially conflicting experimental results could potentially be the identification of proliferating cells as the cells that are Ki67 positively staining [3]; Ki67 staining is not a perfect differentiator between TA and FD cells, since some TA cells may not be stained due to the cell-cycle phase they currently are, and thus counted as FD cells [43].

3.1 Insights into the number of stem cells in the crypt

Before turning to study the effects of driver mutations, we discuss the implications of our model on the potential numbers of stem cells in the crypt. We note that there is an ambiguity in the field regarding the number of stem cells per crypt, since lower values for N_0 around 5 have also been reported [6, 44, 45, 46]. We employed our model to investigate if it can provide insight into the likely stem cells number in a crypt. For $N_0 = 5$, our model predicts distributions for the cell populations that are not in agreement with experimental data (Supplementary Information, section S7 and Fig. S4); chi-square goodness of fit test at 5% significance level disproves the hypothesis that experimental data for FD and total cell populations are consistent with the distributions from model results with $N_0 = 5$. Importantly, for $N_0 = 5$, our model predicts coefficients of variation (CV) for all cell populations $\sim 58\%$. This is significantly higher than the values of CV calculated from experimental data (Table 1). Thus, our model results corroborate the experimental findings that there are ~ 15 stem cells per crypt [2, 7, 8, 47, 48].

4 Effects of driver mutations on population dynamics

Having described the steady-state of healthy colonic crypts, we now use model (1) to determine the size and composition of mutated crypts in early stages of colorectal tumorigenesis, i.e. after the acquisition of certain genetic driver mutations such as *APC* and *KRAS*. *APC* inactivating mutation is sufficient for the initiation of early colorectal adenomas [49], and is present in $\sim 80\%$ of human colorectal cancers [50], resulting in the increase in proliferating cell compartment and the total crypt size [51, 52]. *KRAS* activation [53] is present in $\sim 40\%$ of human colorectal cancers and large adenomas [54], while it is often detected in human hyperplastic polyps [55]. Despite the structural alterations, mutated crypts retain the cell hierarchy described for healthy crypts [6, 11, 29].

The main effect of *Kras* mutation is the increase in division rate of stem cells to $r = 1/15\text{h}^{-1}$ [11], while the number of stem cells per crypt remains unaffected [54]. This represents a 60% increase in r compared to wild-type crypts, which divide on average once per day. This increase in stem cell division rate translates to a 60% increase in TA and FD cell populations in our model, and thus a $\sim 60\%$ increase in total crypt size. This prediction is close to the $\sim 65\%$ increase in crypt area observed experimentally [25] for human hyperplastic polyps, and the $\sim 80\%$ increase in the number of proliferating cells per crypt reported [54] in *Kras*-mutant crypts.

APC inactivation has been shown to result in the overpopulation of stem cells in the crypt [22, 29, 45, 56], without an increase in the stem cell division rate [45, 57]. By employing measurements from experiments and a model for stem cell dynamics, it has been inferred that crypts with *APC* inactivation have, on average, 1.6 times more stem cells compared to wild type crypts [29, 45]. Thus, for crypts with *APC* inactivation, we consider 24 stem cells. In our model, the average numbers of TA, FD and total cells per crypt are proportional to the number of stem cells, and thus a 60% increase in stem cell numbers results in 60% increase in the size of TA and FD cell compartments, as well as the total number of cells in a crypt. Experimentally, a proportional increase up to 100% has been observed in both the TA compartment size and total crypt size as a result of *APC* inactivation [58].

Last, it has been experimentally observed [25] that the difference in the average number of mitoses per area between healthy human crypts and crypts from hyperplastic polyps and adenomas is not significant. Non-elevated mitotic index has also been reported for *Apc*-deficient crypts [58]. The average number of mitoses per area is expressed equivalently as the average ratio of proliferating cells to total number of cells, which, in our model, is approximated by $m_{\text{TA}}/N_{\text{tot}} \approx m_{\text{TA}}/(m_{\text{TA}} + m_{\text{FD}}) = \gamma/(d + \gamma)$. Since the values for d and γ remain unchanged, our model predicts the same number of mitoses per area for both healthy and mutant crypts, in agreement with the experimental results.

5 Discussion

In this work, we present a multitype branching process model of cell population dynamics in colonic crypts. The simplicity of model formulation, along with its analytically obtained exact solution, provides insight into the the process by which both healthy and mutated colonic crypts maintain their size. For our model calibration, the only parameter fitting performed is for TA cell differentiation rate d; the remaining parameter values are estimated directly from the relevant literature. More specifically, we estimate d so that the average crypt size predicted by our model coincides with the experimental data. It is noteworthy that this fitting based only on average crypt size results in the predicted probability distributions for TA, FD and total cell populations to agree with experimental data.

Furthermore, the model's stationarity condition is simple, $d > \lambda$, and can also be interpreted as a criterion for malignancy in the process of colorectal carcinogenesis; our model predicts unbounded growth in cell numbers when the acquired mutations result in unregulated divisions of TA cells, with division rate λ exceeding their differentiation rate d. Indeed, in this model, homeostasis is achieved by adjusting the differentiation rate of TA cells. Another aspect of this homeostatic mechanism is that, for varying apoptosis rates, the crypt size distribution stays the same by adjusting the value of d.

A limitation of our model is the assumption that the number N_0 of stem cells is the same in all crypts. Variation in stem cell number is reported as ± 2 cells around its average [8]. We compare our model results with constant $N_0 = 15$ for all crypts, to results where N_0 is allowed to randomly vary from crypt to crypt, with $N_0 = 13 - 17$. The averaged cell population distributions for varying N_0 coincide with the respective distributions for constant N_0 (Supplementary Information, Fig. S3).

Another limitation of the model is that it presupposes the existence of homeostatic mechanisms responsible

for maintaining the number of stem cells in the crypt [8, 11, 39]; thus, it is not an adequate model for crypt cell dynamics under changes in stem cell population, such as the replenishment of their numbers after an acute stem cell loss. It has been observed experimentally [10, 59] that stem cell homeostasis is based on feedback mechanisms, such as the plasticity of early TA cells to obtain stemness again if needed. However, a crypt cell population model that incorporates these mechanisms would be more complex, and it is outside of the scope of the present work.

Data availability: The code and data used to generate the figures of the main paper and Supplementary Information can be downloaded from GitHub at https://github.com/kmamis/stochastic_model_colonic_crypts

Author contributions: K.M. and I.B. designed research; K.M., R.Z. and I.B. performed research; K.M. and I.B. wrote the paper.

Conflict of interest: The authors declare no conflict of interest.

Acknowledgements: This work is supported by the National Science Foundation grant DMS-2045166.

References

[1] Zeki, S. S., Graham, T. A. & Wright, N. A. Stem cells and their implications for colorectal cancer. *Nature Reviews Gastroenterology and Hepatology* **8**, 90–100 (2011).

[2] Yang, J., Axelrod, D. E. & Komarova, N. L. Determining the control networks regulating stem cell lineages in colonic crypts. *Journal of Theoretical Biology* **429**, 190–203 (2017).

[3] Bravo, R. & Axelrod, D. E. A calibrated agent-based computer model of stochastic cell dynamics in normal human colon crypts useful for in silico experiments. *Theoretical Biology and Medical Modelling* **10**, 66 (2013).

[4] Johnston, M. D., Edwards, C. M., Bodmer, W. F., Maini, P. K. & Chapman, S. J. Mathematical modeling of cell population dynamics in the colonic crypt and in colorectal cancer. *Proceedings of the National Academy of Sciences* **104**, 4008–4013 (2007).

[5] Hall, P. A., Coates, P. J., Ansari, B. & Hopwood, D. Regulation of cell number in the mammalian gastrointestinal tract: the importance of apoptosis. *Journal of Cell Science* **107**, 3569–3577 (1994).

[6] Barker, N. *et al.* Crypt stem cells as the cells-of-origin of intestinal cancer. *Nature* **457**, 608–611 (2009).

[7] Gehart, H. & Clevers, H. Tales from the crypt: New insights into intestinal stem cells. *Nature Reviews Gastroenterology and Hepatology* **16**, 19–34 (2019).

[8] Snippert, H. J. *et al.* Intestinal crypt homeostasis results from neutral competition between symmetrically dividing Lgr5 stem cells. *Cell* **143**, 134–144 (2010).

[9] Spit, M., Koo, B. K. & Maurice, M. M. Tales from the crypt: Intestinal niche signals in tissue renewal, plasticity and cancer. *Open Biology* **8**, 180120 (2018).

[10] Clevers, H. The intestinal crypt, a prototype stem cell compartment. *Cell* **154**, 274–284 (2013).

[11] Snippert, H. J., Schepers, A. G., Van Es, J. H., Simons, B. D. & Clevers, H. Biased competition between Lgr5 intestinal stem cells driven by oncogenic mutation induces clonal expansion. *EMBO Reports* **15**, 62–69 (2014).

[12] Van Der Flier, L. G. & Clevers, H. Stem cells, self-renewal, and differentiation in the intestinal epithelium. *Annual Review of Physiology* **71**, 241–260 (2009).

[13] Sanman, L. E. *et al.* Transit-Amplifying cells coordinate changes in intestinal epithelial cell-type composition. *Developmental Cell* **56**, 356–365 (2021).

[14] Giles, R. H., Van Es, J. H. & Clevers, H. Caught up in a Wnt storm: Wnt signaling in cancer. *Biochimica et Biophysica Acta - Reviews on Cancer* **1653**, 1–24 (2003).

[15] Beumer, J., Gehart, H. & Clevers, H. Enteroendocrine dynamics - New tools reveal hormonal plasticity in the gut. *Endocrine Reviews* **41**, 1–12 (2020).

[16] Van Leeuwen, I. M. M., Byrne, H. M., Jensen, O. E. & King, J. R. Crypt dynamics and colorectal cancer: advances in mathematical modelling. *Cell Prolif* **39**, 157–181 (2006).

[17] Carulli, A. J., Samuelson, L. C. & Schnell, S. Unraveling intestinal stem cell behavior with models of crypt dynamics. *Integrative Biology* **6**, 243–257 (2014).

[18] Totafurno, J., Bjerknes, M. & Cheng, H. Variation in crypt size and its influence on the analysis of epithelial cell proliferation in the intestinal crypt. *Biophysical Journal* **54**, 845–858 (1988).

[19] Gerike, T. G., Paulus, U., Potten, C. S. & Loeffler, M. A dynamic model of proliferation and differentiation in the intestinal crypt based on a hypothetical intraepithelial growth factor. *Cell Proliferation* **31**, 93–110 (1998).

[20] Meineke, F. A., Potten, C. S. & Loeffler, M. Cell migration and organization in the intestinal crypt using a lattice-free model. *Cell Proliferation* **34**, 253–266 (2001).

[21] Van Leeuwen, I. M. *et al.* An integrative computational model for intestinal tissue renewal. *Cell Proliferation* **42**, 617–636 (2009).

[22] Boman, B. M., Fields, J. Z., Bonham-Carter, O. & Runquist, O. A. Computer modeling implicates stem cell overproduction in colon cancer initiation. *Cancer Research* **61**, 8408–8411 (2001).

[23] Dingli, D., Traulsen, A. & Pacheco, J. M. Compartmental architecture and dynamics of hematopoiesis. *PLoS ONE* **2**, e345 (2007).

[24] Lo, W. C. *et al.* Feedback regulation in multistage cell lineages. *Mathematical Biosciences and Engineering* **6**, 59–82 (2009).

[25] Wong, W. M. *et al.* Histogenesis of human colorectal adenomas and hyperplastic polyps: The role of cell proliferation and crypt fission. *Gut* **50**, 212–217 (2002).

[26] Tomlinson, I. P. M. & Bodmer, W. F. Failure of programmed cell death and differentiation as causes of tumors: Some simple mathematical models (tumorigenesis/apoptosis). *Proceedings of the National Academy of Sciences* **92**, 11130–11134 (1995).

[27] Paulus, U., Potten, C. S. & Loeffler, M. A model of the control of cellular regeneration in the intestinal crypt after perturbation based solely on local stem cell regulation. *Cell Prolif* **25**, 559–578 (1992).

[28] Bozic, I. Quantification of the selective advantage of driver mutations is dependent on the underlying model and stage of tumor evolution. *Cancer Research* **82**, 21–24 (2022).

[29] Baker, A. M. *et al.* Quantification of crypt and stem cell evolution in the normal and neoplastic human colon. *Cell Reports* **8**, 940–947 (2014).

[30] Kimmel, M. & Axelrod, D. E. *Branching Processes in Biology* (Springer, New York Berlin Heidelberg, 2002).

[31] Zhang, R., Ukogu, O. A. & Bozic, I. Waiting times in a branching process model of colorectal cancer initiation. *bioRxiv* **2022.06.22.497226** (2022).

[32] Bozic, I. & Wu, C. J. Delineating the evolutionary dynamics of cancer from theory to reality. *Nature cancer* **1**, 580–588 (2020).

[33] Bozic, I. *et al.* Accumulation of driver and passenger mutations during tumor progression. *Proceedings of the National Academy of Sciences* **107**, 18545–18550 (2010).

[34] Antal, T. & Krapivsky, P. L. Exact solution of a two-type branching process: Models of tumor progression. *Journal of Statistical Mechanics: Theory and Experiment* **2011**, P08018 (2011).

[35] Avanzini, S. *et al.* A mathematical model of ctDNA shedding predicts tumor detection size. *Sci. Adv* **6**, eabc4308 (2020).

[36] Clayton, E. *et al.* A single type of progenitor cell maintains normal epidermis. *Nature* **446**, 185–189 (2007).

[37] Antal, T. & Krapivsky, P. L. Exact solution of a two-type branching process: Clone size distribution in cell division kinetics. *Journal of Statistical Mechanics: Theory and Experiment* **2010**, P07028 (2010).

[38] Shahriyari, L. & Komarova, N. L. Symmetric vs. asymmetric stem cell divisions: an adaptation against cancer? *PloS one* **8**, e76195 (2013).

[39] Lopez-Garcia, C., Klein, A. M., Simons, B. D. & Winton, D. J. Intestinal stem cell replacement follows a pattern of neutral drift. *Science* **330**, 822–825 (2010).

[40] Leblond, C. P. Classification of cell populations on the basis of their proliferative behavior. In Congdon, C. C. & Mori-Chavez, P. (eds.) *Control of Cell Division and the Induction of Cancer*, 119–150 (National Cancer Institute, Bethesda, MD, 1964).

[41] Potten, C. S. & Loeffler, M. Stem cells: attributes, cycles, spirals, pitfalls and uncertainties Lessons for and from the Crypt. *Development* **110**, 1001–1020 (1990).

[42] Bjerknes, M. & Cheng, H. The stem-cell zone of the small intestinal epithelium. IV. Effects of resecting 30% of the small intestine. *The American Journal of Anatomy* **160**, 93–103 (1981).

[43] Miller, I. *et al.* Ki67 is a graded rather than a binary marker of proliferation versus quiescence. *Cell Reports* **24**, 1105–1112 (2018).

[44] Sato, T. *et al.* Single Lgr5 stem cells build crypt-villus structures in vitro without a mesenchymal niche. *Nature* **459**, 262–265 (2009).

[45] Kozar, S. *et al.* Continuous clonal labeling reveals small numbers of functional stem cells in intestinal crypts and adenomas. *Cell stem cell* **13**, 626–633 (2013).

[46] Vermeulen, L. *et al.* Defining stem cell dynamics in models of intestinal tumor initiation. *Science* **342**, 995–998 (2013).

[47] Ritsma, L. *et al.* Intestinal crypt homeostasis revealed at single-stem-cell level by in vivo live imaging. *Nature* **507**, 362–365 (2014).

[48] Nicolas, P., Kim, K. M., Shibata, D. & Tavaré, S. The stem cell population of the human colon crypt: Analysis via methylation patterns. *PLoS Computational Biology* **3**, 0364–0374 (2007).

[49] Lamlum, H. *et al.* APC mutations are sufficient for the growth of early colorectal adenomas. *Proceedings of the National Academy of Sciences* **97**, 2225–2228 (2000).

[50] van Neerven, S. M. *et al.* Apc-mutant cells act as supercompetitors in intestinal tumour initiation. *Nature* **594**, 436–441 (2021).

[51] Dow, L. E. *et al.* Apc restoration promotes cellular differentiation and reestablishes crypt homeostasis in colorectal cancer. *Cell* **161**, 1539–1552 (2015).

[52] Boman, B. M. *et al.* Colonic crypt changes during adenoma development in familial adenomatous polyposis. Immunohistochemical evidence for expansion of the crypt base cell population. *Am J Pathol* **165**, 1489–1498 (2004).

[53] Paterson, C., Clevers, H. & Bozic, I. Mathematical model of colorectal cancer initiation. *Proceedings of the National Academy of Sciences* **117**, 20681–20688 (2020).

[54] Feng, Y. *et al.* Mutant kras promotes hyperplasia and alters differentiation in the colon epithelium but does not expand the presumptive stem cell pool. *Gastroenterology* **141**, 1003–1013 (2011).

[55] Chan, T. L., Zhao, W., Leung, S. Y. & Yuen, S. T. BRAF and KRAS mutations in colorectal hyperplastic polyps and serrated adenomas. *Cancer Research* **63**, 4878–4881 (2003).

[56] Zhang, T. *et al.* APC mutations in human colon lead to decreased neuroendocrine maturation of ALDH+ stem cells that alters GLP-2 and SST feedback signaling: Clue to a link between WNT and retinoic acid signalling in colon cancer development. *PLoS ONE* **15**, e0239601 (2020).

[57] Bruschi, M. *et al.* Loss of Apc rapidly impairs DNA methylation programs and cell fate decisions in Lgr5+ intestinal stem cells. *Cancer Research* **80**, 2101–2113 (2020).

[58] Sansom, O. J. *et al.* Myc deletion rescues Apc deficiency in the small intestine. *Nature* **446**, 676–679 (2007).

[59] Clevers, H., Loh, K. M. & Nusse, R. An integral program for tissue renewal and regeneration: Wnt signaling and stem cell control. *Science* **346** (2014).